Supplemental Material for Correlation between Length and Tilt of Lipid Tails

Dmitry I. Kopelevich and John F. Nagle

I. RESULTS FOR ALTERNATIVE DIRECTOR DEFINITIONS

A. Alternative Director Definitions

The goal of this section is to investigate the tilt-length correlations for the following alternative definitions of the tail director:

A. Molecular directors, which characterize tilt of an entire molecule, rather than an individual tail. This approach to the director definition was taken in the earlier work [1–3]. Here, we investigate two different definitions of molecular directors (see Fig. S1a):

1. Mean tail director $\mathbf{n}_m$, defined as the average of the end-to-end directors $\overrightarrow{\mathrm{C}_N\mathrm{C}_1}$ of individual tails of a molecule. Specifically, $\mathbf{n}_m$ is defined as the vector pointing from $\mathrm{C}_N^{(m)}$ to $\mathrm{C}_1^{(m)}$, where $\mathrm{C}_i^{(m)}$ is the midpoint between atoms C_i of different tails of a lipid molecule.

2. Overall molecular director $\mathbf{n}_P$, which accounts for contributions of both the head- and tail-groups to molecular tilt. Following [3], we define $\mathbf{n}_P$ as the vector pointing from $\mathrm{C}_N^{(m)}$ to the phosphorus atom in the lipid head-group.

Similarly to the individual tail directors, the length L of a molecular director is defined as the distance between its end-points.

B. Gyration director $\mathbf{n}_g$ defined as the principal direction of gyration of a lipid tail corresponding to its largest radius of gyration. In the calculations of the tensor of gyration $\mathbf{S}$ of a hydrocarbon chain, we neglect hydrogen atoms belonging to the chain, i.e.

$$\mathbf{S} = \frac{1}{N}\sum_{k=1}^{N}(\mathbf{r}_k - \mathbf{r}_C)\otimes(\mathbf{r}_k - \mathbf{r}_C), \tag{1}$$

where the summation is performed over the chain carbon atoms, $\mathbf{r}_C$ is the center of mass of these atoms, and $\mathbf{r}_k$ is the position of the k-th atom. Furthermore, we require that the gyration director passes through $\mathbf{r}_C$. The length L_g

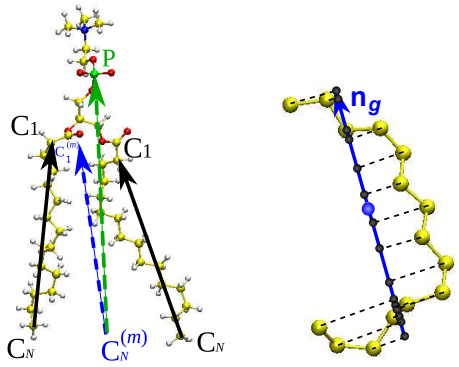

(a) (b)

Figure S1. (a) End-to-end directors of individual lipid tails (solid arrows) and the molecular directors $\mathbf{n}_m$ (blue dashed arrow) and $\mathbf{n}_P$ (green dashed arrow). Spheres of different colors represent atoms of different elements: yellow = C, white = H, red = O, green = P, blue = N. (b) Gyration director of a hydrocarbon chain. For clarity, only carbon carbon atoms of the chain are shown (yellow spheres); the black spheres represent projections of the positions of the carbon atoms onto the gyration director. The blue sphere represents the chain center of mass.

of $\mathbf{n}_g$ is defined as the end-to-end length of the chain formed by the projections of the carbon atoms onto $\mathbf{n}_g$ (see Fig. S1b), i.e.

$$L_g = \max_k(\mathbf{r}_k - \mathbf{r}_C)\cdot\hat{\mathbf{n}}_g - \min_k(\mathbf{r}_k - \mathbf{r}_C)\cdot\hat{\mathbf{n}}_g, \tag{2}$$

where $\hat{\mathbf{n}}_g = \mathbf{n}_g/|\mathbf{n}_g|$ is the normalized gyration director.

Although radii of gyration are often used to characterize macromolecular shapes [4–6], the property of the tensor of gyration most relevant to this work appears to be little known. Specifically, line $l_{\min}$, defined as having the smallest mean-square displacement (MSD) from a group of atoms, contains the gyration director $\mathbf{n}_g$ of this group. To prove this, let us consider a group of N atoms with coordinates $\mathbf{r}_k$ and obtain line $l_{\min}$ with the smallest MSD from these atoms,

$$\Delta^2 = \frac{1}{N}\sum_{k=1}^{N}\Delta_k^2 \to \min. \tag{3}$$

Here, Δ_k is the distance from the k-th atom to the line. Define this line generally as being directed along unit vector $\hat{\mathbf{u}}$ and passing through some point with coordinates given by vector $\mathbf{r}_0$. Then

$$\Delta_k^2 = |\mathbf{r}_k - \mathbf{r}_0|^2 - [(\mathbf{r}_k - \mathbf{r}_0)\cdot\hat{\mathbf{u}}]^2. \tag{4}$$

Let us now consider a system of coordinates with the origin at the center of mass, $\sum_k \mathbf{r}_k = 0$. Then Eqs. (3), (4) yield:

$$\Delta^2 = \frac{1}{N}\sum_{k=1}^{N}|\mathbf{r}_k|^2 + \left[|\mathbf{r}_0|^2 - (\mathbf{r}_0\cdot\hat{\mathbf{u}})^2\right] - \hat{\mathbf{u}}^T\mathbf{S}\hat{\mathbf{u}}. \tag{5}$$

The first term in (5) is independent of $\mathbf{r}_0$ and $\hat{\mathbf{u}}$. The terms contained in the square brackets represent the difference between the squared lengths of the vector $\mathbf{r}_0$ and the projection of this vector onto $\hat{\mathbf{u}}$. This difference is minimized if $\mathbf{r}_0$ is parallel to $\hat{\mathbf{u}}$, i.e. line $l_{\min}$ passes through the origin (center of mass). Finally, to minimize Δ^2, the unit vector $\hat{\mathbf{u}}$ should maximize $\hat{\mathbf{u}}^T\mathbf{S}\hat{\mathbf{u}}$, i.e. $\hat{\mathbf{u}}$ is an eigenvector corresponding to the largest radius of gyration. Hence, line $l_{\min}$ contains the gyration director.

B. Analysis Results

Dependence of the mean director length $\bar{L}(m)$ on tilt m for all considered director definitions is shown in Fig. S2. In all cases, increasing tilt leads to a slight decrease in $\bar{L}(m)$. Moreover, $\bar{L}(m)$ for the end-to-end and gyration tail directors are nearly identical and the normalized lengths $\bar{L}(m)/\bar{L}(0)$ of both considered molecular directors, $\mathbf{n}_m$ and $\mathbf{n}_P$, exhibit a very similar dependence on tilt. The latter observation suggests that the tilt-induced lipid shortening is dominated by shortening of tails, with head-groups making a negligible contribution.

The conditional distributions $P(L|m)$ of the directors $\mathbf{n}_m$, $\mathbf{n}_P$, and $\mathbf{n}_g$ are shown in Fig. S3. These distributions exhibit behavior similar to that of the end-to-end tail directors $\overrightarrow{\mathrm{C}_N\mathrm{C}_1}$ considered in the paper: as tilt increases, the distributions become slightly wider and their peak shifts towards smaller L.

II. 2-ROD MODEL

A. Validation of the 2-rod Model for the DLPC bilayer

In this section, we present evidence that the mechanism of the tilt-induced tail shortening discussed in Section V of the paper is applicable to other saturated lipids. To this end, we repeated the analysis of Section V for a DLPC lipid bilayer. Results of this analysis are summarized in Figures S4 and S5. Qualitative similarity between the DLPC and DPPC results indicate that the 2-rod model holds for a wide class of saturated PC lipids. Moreover, since effect of the head-group in the lipid shortening is negligible (see Fig. S2), it is likely that the conclusions of this paper hold for saturated lipids with different head-groups.

In the remainder of this section, we report additional analysis in support of the 2-rod model. Results of this analysis are the same for the DPPC and DLPC bilayers. Hence, unless stated otherwise, only data for the DPPC bilayer are shown.

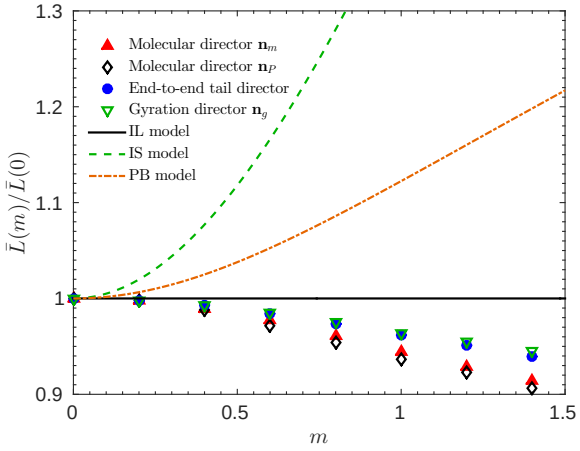

Figure S2. Dependence of the average tail director length $\bar{L}$ on its tilt m for different director definitions. In this plot, $\bar{L}(m)$ is normalized to its value at zero tilt: $\bar{L}(0) = 1.42$ nm for the molecular directors $\mathbf{n}_m$, $\bar{L}(0) = 1.97$ nm for the molecular directors $\mathbf{n}_P$, and $\bar{L}(0) = 1.52$ nm for both the end-to-end and gyration directors of individual tails. The standard errors of the shown $\bar{L}(m)$ do not exceed 0.01 nm.

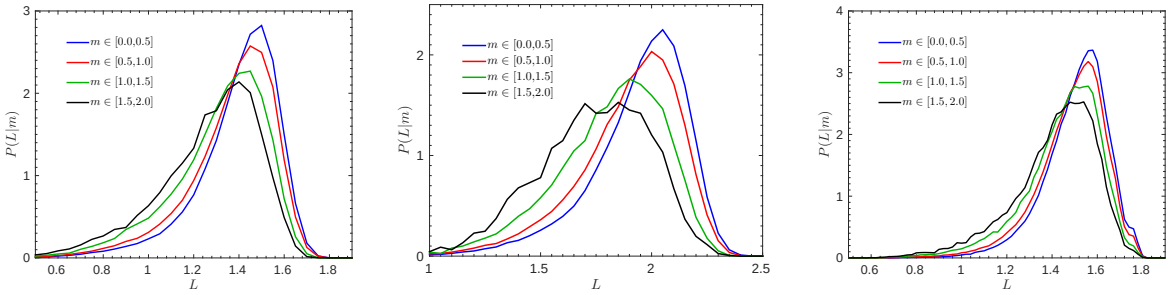

(a) (b) (c)

Figure S3. Conditional probabilities $P(L|m)$ of the length L of (a) molecular directors $\mathbf{n}_m$, (b) molecular directors $\mathbf{n}_P$, and (c) gyration directors $\mathbf{n}_g$.

B. Gyration Director

In this section we demonstrate that conclusions of Section V of the paper hold for the gyration tail director defined in Section I of SM. The hinge point of the 2-rod model is defined here as the position of the chain carbon atom C_h located farthest from the gyration director. Gyration directors $\mathbf{n_1}$ and $\mathbf{n_2}$ of the chain segments C_1-C_h and C_h-C_N are defined similarly to the gyration director of the entire chain. As in the case of the end-to-end directors, the average angle between the gyration directors $\mathbf{n_1}$ and $\mathbf{n_2}$ of the chain segments decreases as the tilt m of the overall tail director $\mathbf{n}$ increases, see Fig. S6. In addition, Fig. S7 indicates that dependence of the mean director lengths on the tilts m and m_1 of the gyration directors $\mathbf{n}$ and $\mathbf{n_1}$ is qualitatively the same as that for the end-to-end directors (see Fig. 6 of the paper).

C. Additional Validation

The two-rod model is useful only if it provides a more accurate representation of the tail shape than the single-rod model assumed in the existing theories. To compare accuracy of the single- and two-rod models, we obtain the mean deviation of the chain carbon atoms from the overall chain director $\mathbf{n}$ and the directors $\mathbf{n_1}$ and $\mathbf{n_2}$ of the chain segments C_1-C_h and C_h-C_N (C_h is the hinge atom). Specifically, we compute the root mean square displacement (RMSD) of carbon atoms from the directors,

$$\Delta(\mathbb{n}) = \sqrt{\frac{\sum_{i=i_1}^{i_2} \Delta_i^2(\mathbb{n})}{i_2 - i_1 + 1}}. \tag{6}$$

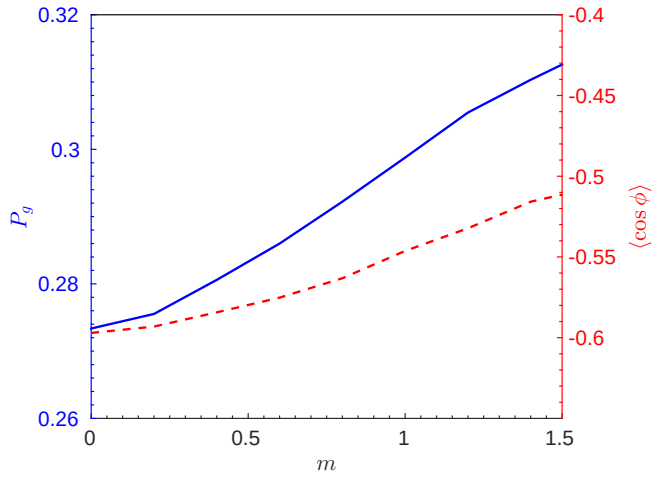

Figure S4. Same as Fig. 4 of the paper but for the DLPC bulayer.

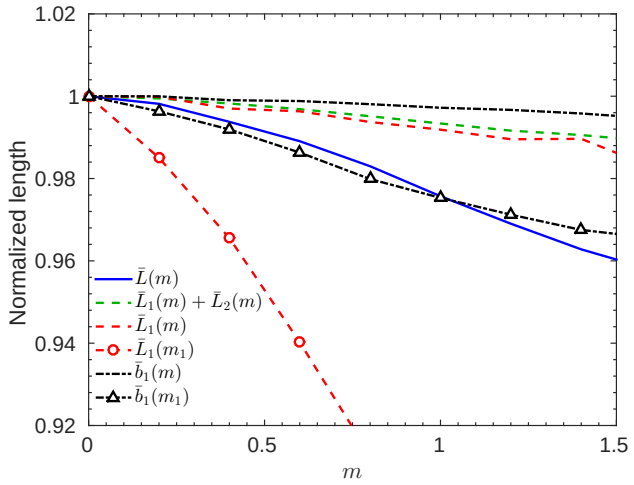

Figure S5. Same as Fig. 6 of the paper but for the DLPC bilayer. Here, the normalization values are $\bar{L}(m=0) = 1.11$ nm, $\bar{L}_1(m=0) = 0.63$ nm, $\bar{L}_2(m=0) = 0.60$ nm, $\bar{L}_1(m_1=0) = 0.67$ nm, and $\bar{b}_1(m=0) = \bar{b}_1(m_1=0) = 0.10$ nm.

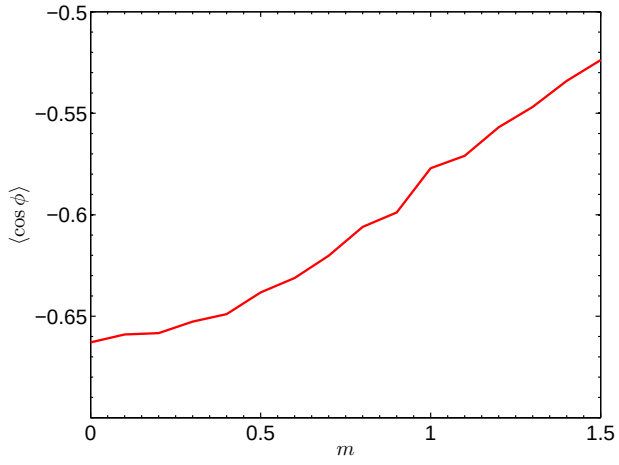

Figure S6. Average relative orientation $\langle\cos\phi\rangle$ of the gyration directors $\mathbf{n_1}$ and $\mathbf{n_2}$ of the tail segments versus tilt m of the overall tail director $\mathbf{n}$.

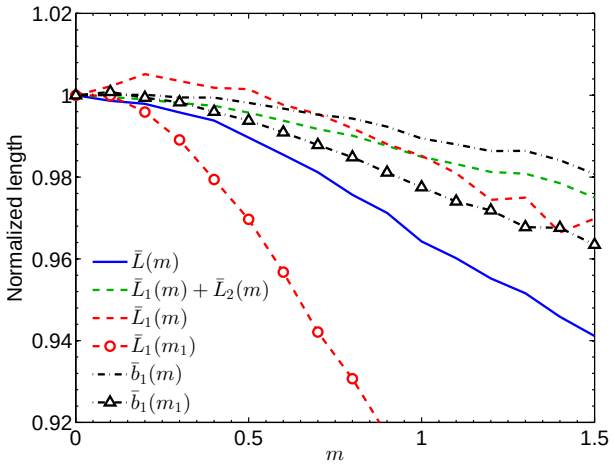

Figure S7. Same as Fig. 6 of the paper but for the gyration directors. Here, the normalization values are $\bar{L}(m=0) = 1.52$ nm, $\bar{L}_1(m=0) = 0.85$ nm, $\bar{L}_2(m=0) = 0.80$ nm, $\bar{L}_1(m_1=0) = 0.90$ nm, and $\bar{b}_1(m=0) = \bar{b}_1(m_1=0) = 0.10$ nm.

Table S1. Root mean square displacements $\bar{\Delta}(\mathbb{n}, 0)$ of atoms from the overall tail director $\mathbf{n}$ and the directors $\mathbf{n_1}$ and $\mathbf{n_2}$ of the tail segments C_1-C_h and C_h-C_N at zero tail tilt. Data for both DPPC and DLPC bilayers are shown.

Lipid	Director type	$\bar{\Delta}(\mathbf{n}, 0)$	$\bar{\Delta}(\mathbf{n_1}, 0)$	$\bar{\Delta}(\mathbf{n_2}, 0)$
DPPC	End-to-end	1.9 Å	1.0 Å	1.0 Å
	Gyration	1.1 Å	0.6 Å	0.6 Å
DLPC	End-to-end	1.5 Å	0.8 Å	0.8 Å
	Gyration	0.9 Å	0.5 Å	0.5 Å

Here, $\mathbb{n}$ represents one of the directors ($\mathbb{n} = \mathbf{n}$, $\mathbf{n_1}$, or $\mathbf{n_2}$), $\Delta_i(\mathbb{n})$ is the distance between atom C_i and director $\mathbb{n}$. For the end-to-end directors, the summation is performed over all carbon atoms in the chain (or the chain segment) excluding the chain (segment) end-points, i.e.

$$\begin{cases} i_1 = 2,\ i_2 = N-1 \text{ for } \mathbb{n} = \mathbf{n}, \\ i_1 = 2,\ i_2 = h-1 \text{ for } \mathbb{n} = \mathbf{n_1}, \text{ and} \\ i_1 = h+1,\ i_2 = N-1 \text{ for } \mathbb{n} = \mathbf{n_2}. \end{cases} \tag{7}$$

For the gyration directors, the end-points are included in the summation, since these points do not necessarily lie on the directors. The RMSDs for individual chains are ensemble averaged to obtain mean RMSDs, $\bar{\Delta}(\mathbb{n}, m)$, corresponding to different chain tilts m.

The RMSDs of chains with zero tilt are listed in Table S1. Not surprisingly, the RMSDs are smaller for the gyration directors. Nevertheless, for both considered types of the directors, the 2-rod model yields a better approximation to the chain shape, as evidenced by the substantial difference between the overall tail directors, $\bar{\Delta}(\mathbf{n}, m)$, and the directors of the individual rods, $\bar{\Delta}(\mathbf{n_1}, m)$ and $\bar{\Delta}(\mathbf{n_2}, m)$ of the 2-rod model. If the tail shape were statistically a single cylinder, the RMSDs of the 2-rod model would be only marginally smaller than the single-rod RMSD.

Effect of the chain tilt on the RMSDs is shown in Fig. S8. While all RMSDs grow with increasing tilt, the RMSDs of the 2-rod model do not grow as fast as those of the single-rod model, which indicates that the single-rod approximation becomes even less accurate as the tail tilt increases.

D. Distribution of Gauche Rotamers in Lipid Tails

The purpose of this section is to connect the 2-rod model for lipid tails with distribution of gauche rotamers along the tails. To this end, we compute (i) the fraction $P_{g,h}$ of gauche rotamers in dihedral angles with the hinge atom C_h in the central bond and (ii) the fractions $P_{g,1}$ and $P_{g,2}$ of gauche rotamers in the interior of segments C_1-C_h and C_h-C_N. I.e., dihedral angle C_i-C_{i+1}-C_{i+2}-C_{i+3} contributes to $P_{g,h}$ if $i = h-2$ or $i = h-1$, to $P_{g,1}$ if $i < h-2$, and to $P_{g,2}$ if $i > h-1$.

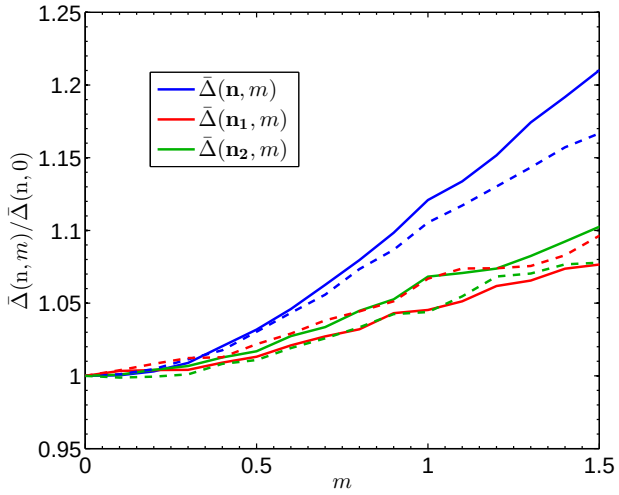

Figure S8. Effect of the chain tilt on the RMSDs of carbon atoms from the overall tail director $\mathbf{n}$ and the rod directors $\mathbf{n_1}$ and $\mathbf{n_2}$. RMSDs corresponding to end-to-end and gyration directors are shown by solid and dashed lines, respectively. The plotted RMSDs are normalized to their values at zero tilt.

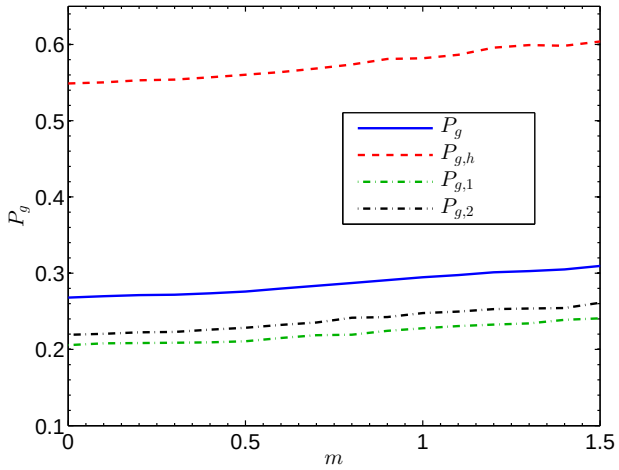

Figure S9. Fraction of gauche rotamers versus tilt m in the entire tail (P_g), at the hinge atom ($P_{g,h}$), and in the segments C_1-C_h and C_h-C_N ($P_{g,1}$ and $P_{g,2}$, respectively).

The dependence of $P_{g,h}$, $P_{g,1}$, and $P_{g,2}$ on the chain tilt is shown in Fig. S9. For comparison, the fraction $P_g(m)$ of the gauche rotamers in the entire chain is also shown. The data shown in Fig. S9 were obtained using the end-to-end tail director $\overrightarrow{C_N C_1}$ to identify the hinge atom C_h. The gyration director yields nearly identical results (data not shown).

It is evident from Fig. S9 that a dihedral angle containing the hinge atom C_h is more likely to be in gauche than trans conformation even at zero chain tilt. On the other hand, the fraction of the gauche conformations inside the segments C_1-C_h and C_h-C_N is smaller than the average fraction for the entire chain. This is in agreement with the relative insensitivity of the segment length per methylene group, $\bar{b}_1$ and $\bar{b}_2$, to the chain tilt (see Fig. 6 in the paper and Fig. S7 in SM).

III. TILT-LENGTH CORRELATION PREDICTED BY THE CONTINUUM MODEL FOR LIPID BILAYERS

In section IV of the paper it is shown that the continuum model for a single monolayer predicts zero correlation between the chain length and tilt. We now turn from monolayers to bilayers and investigate the effect of monolayer coupling on the tilt-length correlation.

The total bilayer energy is the sum of energies $F_{\rm W}$ of individual monolayers [see Eq. (21) of the paper] and the energy $F_{\rm coupl}$ of coupling between the monolayers. Assume harmonic coupling,

$$F_{\rm coupl} = \frac{k_m}{2}(z_m^{(1)} - z_m^{(2)})^2, \tag{8}$$

where k_m is the coupling strength, the superscript (α) indicates the monolayer number ($\alpha = 1, 2$; $\alpha = 1$ corresponds to the upper monolayer), and $z_m^{(\alpha)}$ is the surface passing through end-points of lipid tails of the α-th monolayer. Up to the required accuracy,

$$z_m^{(\alpha)} = z^{(\alpha)} + (-1)^\alpha L^{(\alpha)}, \tag{9}$$

where $z^{(\alpha)}(x, y)$ is the dividing surface of the α-th monolayer, i.e. surface separating the lipid head- and tail-groups. It is convenient to introduce symmetric and antisymmetric modes,

$$z^+ = \frac{z^{(1)} + z^{(2)}}{2}, \quad z^- = \frac{z^{(1)} - z^{(2)} - 2L_0}{2}, \tag{10}$$

$$l^+ = \frac{l^{(1)} + l^{(2)}}{2}, \quad l^- = \frac{l^{(1)} - l^{(2)}}{2}. \tag{11}$$

Then

$$F_{\rm coupl} = 2k_m(z^- - L_0 l^+)^2. \tag{12}$$

The z-components of the tilt and director vectors do not contribute to the quadratic approximation to the monolayer free energy [Eq. (21) of the paper] and it is thus sufficient to consider two-dimensional vectors $\mathbf{m} = (m_x, m_y)$ and $\mathbf{n} = (n_x, n_y)$. Up to the required accuracy, these vectors are related by the following equation:

$$\mathbf{n}^{(\alpha)} = \mathbf{m}^{(\alpha)} + (-1)^{\alpha+1}\nabla z^{(\alpha)}, \tag{13}$$

It then follows that

$$\mathbf{n}^+ = \mathbf{m}^+ + \nabla z^- \quad \text{and} \quad \mathbf{n}^- = \mathbf{m}^- + \nabla z^+, \tag{14}$$

where

$$\mathbf{m}^+ = \frac{\mathbf{m}^{(1)} + \mathbf{m}^{(2)}}{2}, \quad \mathbf{m}^- = \frac{\mathbf{m}^{(1)} - \mathbf{m}^{(2)}}{2}, \tag{15}$$

$$\mathbf{n}^+ = \frac{\mathbb{n}^{(1)} + \mathbb{n}^{(2)}}{2}, \quad \mathbf{n}^- = \frac{\mathbb{n}^{(1)} - \mathbb{n}^{(2)}}{2} \tag{16}$$

$$\tag{17}$$

are the symmetric and antisymmetric components of the vectors $\mathbf{m}$ and $\mathbf{n}$.

The total bilayer energy can then be written as

$$\begin{aligned} F_{\rm b} &= F_{\rm W}(\mathbf{n}^{(1)}, \mathbf{m}^{(1)}, l^{(1)}) + F_{\rm W}(\mathbf{n}^{(2)}, \mathbf{m}^{(2)}, l^{(2)}) + F_{\rm coupl} \\ &= 2F_{\rm W}(\mathbf{n}^-, \mathbf{m}^-, l^-) + G(z^-, \mathbf{m}^+, l^+), \end{aligned} \tag{18}$$

where

$$G(z^-, \mathbf{m}^+, l^+) = 2\left[F_{\rm W}(\nabla z^- + \mathbf{m}^+, \mathbf{m}^+, l^+) + k_m(z^- - L_0 l^+)^2\right]. \tag{19}$$

The variables $(\mathbf{n}^-, \mathbf{m}^-, l^-)$ are decoupled from $(z^-, \mathbf{m}^+, l^+)$. Furthermore, up to the factor of two, the free energy of $(\mathbf{n}^-, \mathbf{m}^-, l^-)$ is the same as that of a single monolayer. Hence, l^- is decoupled from the tilt modes. However, l^+ may be coupled with the tilt modes $\mathbf{m}^+$ because the monolayer-monolayer interactions introduce coupling between l^+ and z^- and z^- is coupled with $\mathbf{m}^+$ through the $(\nabla \cdot \mathbf{n}^+)^2$ term in $F_{\rm W}$.

Eq.(18) is a slight generalization of the expression for the free energy developed by Watson et al. [2] where it was assumed that $z_m^{(1)} = z_m^{(2)} = z_m$, i.e. $k_m \to \infty$. In this case, $l^+ = z^-/L_0$ and $l^- = -\epsilon/L_0$, where $\epsilon \equiv z_m - z^+$. In the remainder of this section we assume that $k_m = \infty$, i.e. $G(z^-, \mathbf{m}^+) = 2F_{\rm W}(\nabla z^- + \mathbf{m}^+, \mathbf{m}^+, z^-/L_0)$. It is shown in Section IV that finite k_m yields similar results.

Fourier transforms of the bilayer degrees of freedom are defined by

$$g_{\mathbf{q}} = \frac{1}{\sqrt{A_p}} \int g(\mathbf{r}) e^{-i\mathbf{q}\cdot\mathbf{r}} d\mathbf{r}, \quad g(\mathbf{r}) = \frac{1}{\sqrt{A_p}} \sum_{\mathbf{q}} g_{\mathbf{q}} e^{i\mathbf{q}\cdot\mathbf{r}}, \tag{20}$$

where $\mathbf{r} = (x, y)$, $\mathbf{q} = (q_x, q_y)$ is the wavevector, A_p is the area of the membrane projection onto the $x - y$ plane, and the relevant $g(\mathbf{r})$ are $z^-(\mathbf{r})$, $m^{||}(\mathbf{r})$, and $l^+(\mathbf{r})$. Here, $m^{||}(\mathbf{r})$ is the longitudinal (curl-free) component of the tilt vector field $\mathbf{m}^+$. The Fourier transform of $m^{||}(\mathbf{r})$ corresponds to the projection of $\mathbf{m}^+_{\mathbf{q}}$ on $\mathbf{q}$. Following [2] we omit the contribution of the transverse (divergence-free) component of $\mathbf{m}^+$ to the free energy since it is decoupled from other degrees of freedom of the bilayer.

Performing Fourier transform of $G(z^-, \mathbf{m}^+)$ and integrating over the entire bilayer yields [2]

$$G = \sum_{\mathbf{q}} \mathbf{f}^*_{\mathbf{q}} \mathbf{B}_{\mathbf{q}} \mathbf{f}_{\mathbf{q}}, \tag{21}$$

where

$$\mathbf{f}_{\mathbf{q}} = (z^-_{\mathbf{q}}, m^{||}_{\mathbf{q}}), \tag{22}$$

the asterisk denotes adjoint matrix, and

$$\mathbf{B}_{\mathbf{q}} = \begin{bmatrix} (\kappa q^4 - q^2\Omega/L_0 + k_A/L_0^2) & -iq(\kappa q^2 - \Omega/2L_0) \\ iq(\kappa q^2 - \Omega/2L_0) & \kappa q^2 + \kappa_\theta \end{bmatrix} \tag{23}$$

is the force matrix. The covariance between the longitudinal tilt component $m^{||}_{\mathbf{q}}$ and the chain length is

$$\langle (l^+)^*_{\mathbf{q}'} m^{||}_{\mathbf{q}} \rangle = \delta_{\mathbf{q},\mathbf{q}'} \frac{k_B T}{2L_0} (\mathbf{B}^{-1}_{\mathbf{q}})_{21} = -\delta_{\mathbf{q},\mathbf{q}'} iq\, k_B T c(q^2), \tag{24}$$

where

$$c(q^2) = \frac{\kappa L_0 q^2/2 - \Omega/4}{L_0^2 \kappa \kappa_\theta q^4 + (\kappa k_A - \Omega L_0 \kappa_\theta - \Omega^2/4) q^2 + \kappa_\theta k_A}. \tag{25}$$

The covariance between the chain tilt and length in real space is

$$C^+_{lm}(\mathbf{r}) \equiv \langle l^+(\mathbf{r}_0) \mathbf{m}^+(\mathbf{r}_0 + \mathbf{r}) \rangle = -\frac{k_B T}{A_p} \sum_{\mathbf{q}} i\mathbf{q} c(q^2) e^{i\mathbf{q}\cdot\mathbf{r}} = -\nabla C^+_{l\phi}(\mathbf{r}), \tag{26}$$

where $C^+_{l\phi}(\mathbf{r})$ is the covariance between the tail length l^+ and the scalar potential ϕ^+ of the tilt field $\mathbf{m}^+$ ($-\nabla\phi^+ = \mathbf{m}^{||}$),

$$C^+_{l\phi}(\mathbf{r}) = \frac{k_B T}{A_p} \sum_{\mathbf{q}} c(q^2) e^{i\mathbf{q}\cdot\mathbf{r}} \approx \frac{k_B T}{4\pi^2} \int c(q^2) e^{i\mathbf{q}\cdot\mathbf{r}} d\mathbf{q} = \frac{k_B T}{2\pi} \int_0^\infty c(q^2) J_0(rq) q\, dq. \tag{27}$$

Here, $J_0(r)$ is the Bessel function. The last expression in Eq. (27) emphasizes that $C^+_{l\phi}$ has no azimuthal dependence and, hence, only the r-component of C^+_{lm} is not zero and is equal to

$$C^+_{lm}(r) = -\frac{\partial C^+_{l\phi}(r)}{\partial r} \approx \frac{k_B T}{2\pi} \int_0^{q_{\max}} c(q^2) J_1(rq) q^2\, dq, \tag{28}$$

where $q_{\max}$ is the cut-off wavenumber.

Eq. (28) indicates that coupling between the monolayers induces a long-range correlation between the chain tilt and length. However, since $C^+_{lm}(0) = 0$, this coupling is unlikely to induce correlation between tilt and length of the same chain. Nevertheless, one cannot completely rule this out, since chains are not localized to one value of $\mathbf{r}$ and $C^+_{lm}(r) \neq 0$ for small $r \neq 0$. Therefore, the tilt-length correlation should be considered over a range of values of r corresponding to a tilted chain. E.g., for a tilt angle of 30° and an effective chain length of 12 Å the range for r is 6 Å. Such small values of r are outside of the range of the continuum model. Hence, even though Eq. (28) indicates that $C^+_{lm}(r) \neq 0$ for this r, the specific value of $C^+_{lm}(r)$ is likely different from the one predicted by Eq. (28).

IV. TILT-LENGTH CORRELATION PREDICTED BY THE CONTINUOUS MODEL WITH A HARMONIC COUPLING BETWEEN MONOLAYERS

In section III we investigated the tilt-length correlations assuming infinitely large value of the coupling constant k_m. Here, we apply a similar analysis to the case of finite k_m. In this case, the free energy of the modes $(z^-, \mathbf{m}^+, l^+)$ can be written as

$$G(z^-, \mathbf{m}^+, l^+) = \sum_{\mathbf{q}} \tilde{\mathbf{f}}^*_{\mathbf{q}} \tilde{\mathbf{B}}_{\mathbf{q}} \tilde{\mathbf{f}}_{\mathbf{q}}, \tag{29}$$

where

$$\tilde{\mathbf{f}}_{\mathbf{q}} = (z^-_{\mathbf{q}}, m^{||}_{\mathbf{q}}, l^+_{\mathbf{q}}) \tag{30}$$

and

$$\tilde{\mathbf{B}}_{\mathbf{q}} = \begin{bmatrix} \kappa q^4 + 2k_m & -i\kappa q^3 & -\Omega q^2/2 - 2k_m L_0 \\ i\kappa q^3 & \kappa q^2 + \kappa_\theta & -iq\Omega/2 \\ -\Omega q^2/2 - 2k_m L_0 & iq\Omega/2 & k_A + 2k_m L_0^2 \end{bmatrix}. \tag{31}$$

The covariance between the Fourier modes of the longitudinal component of $\mathbf{m}$ and the chain length is

$$\langle (l^+)^*_{\mathbf{q}'} m^{||}_{\mathbf{q}} \rangle = \delta_{\mathbf{q},\mathbf{q}'} \frac{k_B T}{2} (\tilde{\mathbf{B}}^{-1}_{\mathbf{q}})_{2,3} = -\delta_{\mathbf{q},\mathbf{q}'} iq\, k_B T \tilde{c}(q^2), \tag{32}$$

where

$$\tilde{c}(q^2) = \frac{\kappa L_0 q^2/2 - \Omega/4}{[L_0^2 \kappa\kappa_\theta + \kappa_\theta/2k_m(\kappa k_A - \Omega^2/4)]\, q^4 + (\kappa k_A - \Omega L_0 \kappa_\theta - \Omega^2/4) q^2 + \kappa_\theta k_A} \tag{33}$$

Comparison of Eq. (33) with Eq. (25) reveals that the only effect of finite k_m is a correction to the coefficient in the q^4 term in the denominator. Therefore, finite k_m does not introduce any qualitatively new features to the covariance of the chain length and tilt.

[1] E. R. May, A. Narang, and D. I. Kopelevich, Phys. Rev. E. **76**, 021913 (2007).
[2] M. C. Watson, E. S. Penev, P. M. Welch, and F. L. H. Brown, J. Chem. Phys. **135**, 244701 (2011).
[3] M. C. Watson, E. G. Brandt, P. M. Welch, and F. L. H. Brown, Phys. Rev. Lett. **109**, 028102 (2012).
[4] D. N. Theodorou and U. W. Suter, Macromolecules **18**, 1206 (1985).
[5] V. Blavatska and W. Janke, J. Chem. Phys. **133**, 184903 (2010).
[6] J. Vymětal and J. Vondrášek, J. Phys. Chem. A **115**, 11455 (2011).